THE JOURNAL OF BIOLOGICAL CHEMISTRY VOL. 292, NO. 13, pp. 5216–5226, March 31, 2017

Mutational Analysis of the QRRQ Motif in the Yeast Hig1 Type 2 Protein Rcf1 Reveals a Regulatory Role for the Cytochrome *c* Oxidase Complex*[S]

Received for publication, September 9, 2016, and in revised form, January 12, 2017 Published, JBC Papers in Press, February 6, 2017, DOI 10.1074/jbc.M116.758045

Joshua Garlich[‡], Valentina Strecker[§], Ilka Wittig[§], and Rosemary A. Stuart[‡1]

From the [‡]Department of Biological Sciences, Marquette University, Milwaukee, Wisconsin 53233 and [§]Functional Proteomics, SFB 815 Core Unit, Goethe-Universität, 60590 Frankfurt am Main, Germany

Edited by Dennis R. Voelker

The yeast Rcf1 protein is a member of the conserved family of proteins termed the hypoxia-induced gene (domain) 1 (Hig1 or HIGD1) family. Rcf1 interacts with components of the mitochondrial oxidative phosphorylation system, in particular the cytochrome bc_1 (complex III)-cytochrome *c* oxidase (complex IV) supercomplex (termed III-IV) and the ADP/ATP carrier proteins. Rcf1 plays a role in the assembly and modulation of the activity of complex IV; however, the molecular basis for how Rcf1 influences the activity of complex IV is currently unknown. Hig1 type 2 isoforms, which include the Rcf1 protein, are characterized in part by the presence of a conserved motif, (Q/I)X_3(R/H)XRX_3Q, termed here the QRRQ motif. We show that mutation of conserved residues within the Rcf1 QRRQ motif alters the interactions between Rcf1 and partner proteins and results in the destabilization of complex IV and alteration of its enzymatic properties. Our findings indicate that Rcf1 does not serve as a stoichiometric component, *i.e.* as a subunit of complex IV, to support its activity. Rather, we propose that Rcf1 serves to dynamically interact with complex IV during its assembly process and, in doing so, regulates a late maturation step of complex IV. We speculate that the Rcf1/Hig1 proteins play a role in the incorporation and/or remodeling of lipids, in particular cardiolipin, into complex IV and. possibly, other mitochondrial proteins such as ADP/ATP carrier proteins.

Mitochondria are specialized organelles that are a nexus for several critical cellular pathways, including the aerobic production of energy through oxidative phosphorylation (OXPHOS)[2] (1–4). The enzymes involved in this cellular energy pathway, referred to as complexes I-IV, are embedded within the inner mitochondrial membrane and facilitate the establishment of a proton gradient through the oxidation of reducing equivalents. In the final steps of this process, the electron carrier cytochrome *c* mediates the transfer of electrons from cytochrome bc_1 (complex III) to cytochrome *c* oxidase (COX, complex IV), which donates electrons to O_2, forming water (1, 5–7). The electrochemical proton gradient is utilized by the F_1F_0-ATP synthase and provides the energy necessary to generate ATP from ADP and inorganic phosphate (8). Newly synthesized ATP is then exchanged for cytosolic ADP by the ADP/ATP carrier (AAC) proteins, integral membrane proteins of the mitochondrial inner membrane (9).

OXPHOS enzyme complexes require correct assembly and tight regulation to ensure optimal function and integrity. A point of potential regulation is the organization of OXPHOS enzymes, including AAC and complexes III and IV, into structures termed supercomplexes (1–3, 10–15). These higher-ordered supercomplexes, *e.g.* the III-IV supercomplex, have been proposed to facilitate efficient electron channeling and possibly enable the co-regulation of these enzymes. The III-IV supercomplex is stabilized by the signature mitochondrial phospholipid cardiolipin (CL) and can also include the AAC protein (12, 16–21).

Rcf1 and Rcf2 (respiratory complex factor 1 and 2) are two proteins in the yeast *Saccharomyces cerevisiae* that independently associate with subpopulations of the III-IV supercomplex (22–24). Like the AAC proteins, current data indicate that Rcf1 and Rcf2 support the assembly of complex IV and, thus, III-IV supercomplex organization (12, 22–24). The Rcf1 and Rcf2 proteins have been shown to cooperatively play a critical role in respiration-based growth and influence the activity of complex IV (22–24). The growth defect of the Δ*rcf1;*Δ*rcf2* mutant, at least in part, is caused by a reduction in complex IV enzyme levels in the absence of both Rcf1/Rcf2 proteins (23). Rcf1 physically interacts with the mitochondrially encoded Cox3 subunit during its assembly and has also been shown to modulate the association of Cox12 (Cox6b in mammals) with complex IV enzyme. Cox12 is a peripheral subunit of complex

* This work was supported by National Science Foundation Grant MCB-1157722 and National Institutes of Health Grants R15-GM101594 and R15-GM117551 (to R. A. S.), an Arthur J. Schmitt graduate fellowship award (to J. G.), and by Cluster of Excellence "Macromolecular Complexes" at the Goethe University Frankfurt (DFG Project EXC 115) and SFB815 Project Z1 (to I. W.). The authors declare that they have no conflicts of interest with the contents of this article. The content is solely the responsibility of the authors and does not necessarily represent the official views of the National Institutes of Health.

[S] This article contains supplemental Figure S1.

[1] To whom correspondence should be addressed: Dept. of Biological Sciences, Marquette University, 530 N. 15th St., Milwaukee, WI 53233. Tel.: 414-288-1472; Fax: 414-288-7357; E-mail: rosemary.stuart@marquette.edu.

[2] The abbreviations used are: OXPHOS, oxidative phosphorylation; AAC, ADP/ATP carrier; CL, cardiolipin; BN, blue native; DDM, dodecyl maltoside; Ni-NTA, nickel-nitrilotriacetic acid; CCCP, carbonyl cyanide *p*-chlorophenylhydrazone; DCCD, dicyclohexylcarbodiimide; MBS, *m*-maleimidobenzoyl-*N*-hydroxysuccinimide ester; PG, phosphatidylglycerol; OCR, oxygen consumption rate; TMPD, *N*,*N*,*N*′,*N*′-tetramethyl-*p*-phenylenediamine dihydrochloride.

IV, which, together with Cox2 and Cox3, is involved in the binding of substrate, cytochrome *c*, to complex IV (23, 24). A close association of the Rcf1 and AAC proteins has also been reported (23). It is currently unknown whether the roles of AAC and the Rcf1/Rcf2 proteins in supporting complex IV levels are related and whether they may involve the lipid CL.

Rcf1 and Rcf2 are both members of the conserved protein family termed hypoxia-induced gene 1 family (Hig1) (also referred to as hypoxia-inducible gene domain (HIGD1) family). The Hig1 protein family can largely be divided into two subgroups of isoforms, termed the Hig1 type 1 and the more universally found type 2 isoforms, and the classification of these isoforms is based largely on the presence or absence of a conserved (Q/I)X_3(R/H)XRX_3Q motif (termed here the QRRQ motif), which is characteristically found in Hig1 type 2 family members. The Hig1 type 1 proteins characteristically contain a modified version of this motif, *e.g.* the HIGD1A protein in mammals has (I/V/L)HLIHMRX_3Q instead. Although the Hig1 type 2 isoforms are universally found in all eukaryotes (and in α-proteobacteria) and appear to represent constitutively expressed isoforms, the Hig1 type 1 subgroup is found in higher eukaryotes and appears to represent hypoxia- and stress-induced isoforms (25–27). Rcf1 and Rcf2 are Hig1 type 2 proteins, and *S. cerevisiae*, like many lower eukaryotes (*e.g.* fungi and nematodes), does not contain Hig1 type1 isoforms.

In this study, we have sought to gain further understanding of the significance of Rcf1 involvement with complex IV assembly and its enzymatic properties. We have explored the relevance of the Hig1 type 2 QRRQ motif for the function of yeast Rcf1. As outlined below, our findings indicate that Rcf1 does not act as a subunit of the assembled complex IV enzyme to support its activity, but, rather, we propose that Rcf1 transiently associates with a late-stage assembly intermediate of complex IV to modify it, possibly its lipid composition, and, by doing so, alters its enzymatic properties.

Results

Expression of Rcf1 QRRQ Mutant Derivatives—Rcf1, like the other members of the Hig1 protein family, is an integral inner mitochondrial membrane protein with two predicted transmembrane segments (Fig. 1*A*). A limited sequence alignment illustrates the conserved nature of the QRRQ motif from diverse species, such as in α-proteobacteria, yeast (both Rcf1 and Rcf2), nematodes, and mammals (Fig. 1*B*). In the yeast Rcf1 protein, the QRRQ motif corresponds to residues 61–71, *i.e.* ^{61}QX_3RXRX_3Q^{71} (Fig. 1, *A* and *B*).

The functional significance of the conserved QRRQ motif in the yeast Rcf1 protein was investigated by adopting a strategy of alanine site-directed mutagenesis. Two distinct Rcf1 mutant derivatives were initially created. In the first mutant, glutamines 61 and 71 were simultaneously mutated to alanines to create the *rcf1*^{Q61A,Q71A} derivative. In the second mutant, derivative arginine 67 was mutated to Ala (*rcf1*^{R67A}).

Rcf1 mutant derivatives were expressed as C-terminal His-tagged derivatives in the Rcf1/Rcf2 double-null yeast strain (Δ*rcf1*;Δ*rcf2*). Analysis of isolated mitochondria from the resulting strains revealed that the steady-state levels of the *rcf1*$_{His}^{Q61A,Q71A}$ and *rcf1*$_{His}^{R67A}$ derivatives appeared to be similar to that of the wild-type Rcf1$_{His}$ control, thus indicating that mutation of the QRRQ motif in this manner did not adversely affect the stability of the Rcf1 protein (Fig. 1*C*). The Δ*rcf1*;Δ*rcf2* yeast strain displays a respiration-based growth defect (23). The expression of *rcf1*$_{His}^{Q61A,Q71A}$ and *rcf1*$_{His}^{R67A}$ derivatives, like the Rcf1$_{His}$ wild-type protein, largely complemented the Δ*rcf1*;Δ*rcf2* respiratory growth defect (growth on the non-fermentable carbon source, glycerol) (Fig. 1*D*). This finding indicates that an intact QRRQ motif is not essential for the ability of Rcf1 to support OXPHOS-based yeast growth.

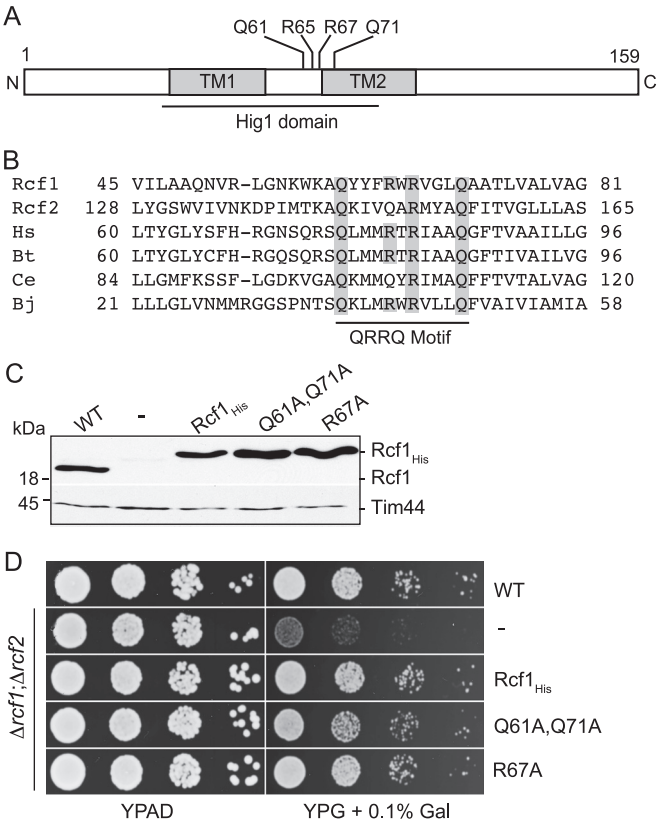

FIGURE 1. **Rcf1, an inner membrane protein and member of Hig1 type 2 family and the conserved QRRQ motif.** *A*, the N_{out}-C_{out} orientation of Rcf1 in the inner membrane with N and C tails exposed to the intermembrane space. The location of QRRQ (Gln^{61}, Arg^{67}, Gln^{61}) motif relative to the two transmembrane segments (*TM1* and *TM2*, respectively) is indicated. *B*, limited sequence alignment (amino acid residue numbers are indicated) of the QRRQ motif region from a selection of Hig1 type 2 family members. *Hs*, *Homo sapiens* (NP_620175); *Bt*, *Bos taurus* (NP_001071329); *Ce*, *C. elegans* (NP_001254152); *Bj*, *Bradyrhizobium japonicum* (WP_014491643). *C*, mitochondria were isolated from the wild type, the Δ*rcf1*;Δ*rcf2* controls (−), or the Δ*rcf1*;Δ*rcf2* strain harboring either His-tagged Rcf1 (Rcf1$_{His}$), *rcf1*$_{His}^{Q61A,Q71A}$ (Gln^{61},Gln^{71}) or *rcf1*$_{His}^{R67A}$ (R67A) derivatives. Rcf1 and Tim44 (control) levels were analyzed by Western blotting. *D*, serial 10-fold dilutions of the WT and Δ*rcf1*;Δ*rcf2* expressing Rcf1$_{His}$, *rcf1*$_{His}^{Q61A,Q71A}$, or *rcf1*$_{His}^{R67A}$ derivatives or not, as indicated, were spotted on YP plates containing glucose (*YPAD*) or glycerol supplemented with 0.1% galactose (*YPG + 0.1% Gal*) and grown at 30 °C.

Expression of rcf1$_{His}^{R67A}$ *Alters the Complex IV Assembly State*—The Δ*rcf1;*Δ*rcf2* mutant mitochondria examined contain reduced levels of complex IV subunits (23). In contrast, the Δ*rcf1;*Δ*rcf2* mitochondria harboring His-tagged wild-type Rcf1 or the *rcf1*$_{His}^{Q61A\ Q71A}$ or *rcf1*$_{His}^{R67A}$ derivatives appeared to have normal steady-state levels of all complex IV subunits analyzed (Fig. 2*A*). We therefore conclude that an intact QRRQ motif does not appear to be required by Rcf1 to support the stable accumulation of complex IV subunits.

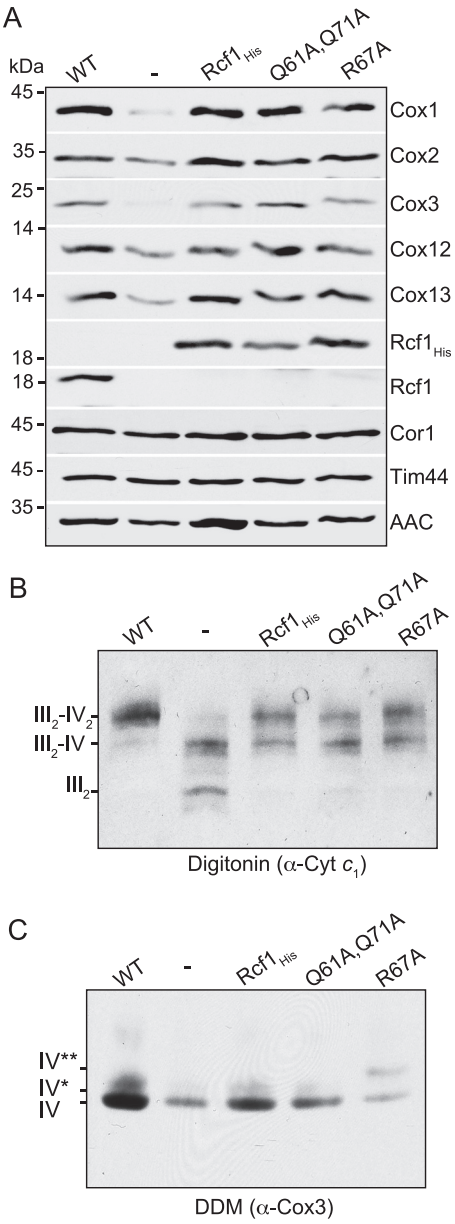

FIGURE 2. **Mutation of the QRRQ motif in Rcf1 affects the stability but not the assembly of complex IV.** *A*, steady-state levels of the OXPHOS subunits in mitochondria (50 μg) isolated from the indicated strains as detailed in Fig. 1*C*. Tim44 was used as a loading control. *B*, mitochondria isolated from the WT and the indicated Δ*rcf1*;Δ*rcf2* strains were solubilized in digitonin (1%) and subjected to BN-PAGE analysis, Western blotting, and immunodecoration with antibodies against the complex III subunit, cytochrome c_1 (α *Cytc*$_1$). *C*, same as in *B*, except that mitochondria were solubilized with DDM (0.6%) prior to BN-PAGE, and decoration was performed with antibodies against the complex IV subunit Cox3 (α-*Cox3*).

Through blue native gel electrophoresis (BN-PAGE), we next addressed whether the QRRQ-mutated derivatives of Rcf1 could support the assembly of complex IV and its association with complex III into the III-IV supercomplex, which is altered in the absence of Rcf1 and Rcf2 (23). In Δ*rcf1;*Δ*rcf2* mitochondria, there is a pronounced shift from the III_2-IV_2 form (observed in the wild-type control mitochondria) to a predominately III_2-IV form and also to free III_2 complexes (Fig. 2*B*), which has been previously attributed to the limiting levels of complex IV in the absence of Rcf1/Rcf2 (23). The III_2-$IV_{(1-2)}$ supercomplex organizational state was largely restored in Δ*rcf1;*Δ*rcf2* mitochondria harboring wild-type $Rcf1_{His}$ (Fig. 2*B*). The *rcf1*$_{His}^{Q61A,Q71A}$ or *rcf1*$_{His}^{R67A}$ mutants, analyzed in parallel, displayed a similar capacity as the wild-type $Rcf1_{His}$ derivative to rescue the organization of the III-IV supercomplex in Δ*rcf1;*Δ*rcf2* mitochondria.

These results indicate that an intact QRRQ motif is not required for the ability of Rcf1 to support the assembly of complex IV and its ability to co-assemble with complex III. Although this conclusion is consistent with the observed steady-state levels of complex IV subunits, which appeared normal in the mitochondria harboring the QRRQ mutant Rcf1 derivatives, we observed a noticeable difference in the behavior of complex IV from *rcf1*$_{His}^{R67A}$ mitochondria when solubilized with the detergent dodecyl maltoside (DDM) prior to the BN-PAGE analysis (Fig. 2*C*). Solubilization of mitochondria with DDM causes complex IV to become physically separated from the III-IV supercomplex assembly, and released complex IV migrates independently as monomers (IV) on the BN-PAGE (24, 28). In wild-type mitochondria, a small fraction of a slightly larger form of complex IV, termed IV*, was also detected and represents the population of monomeric complex IV, where the peripheral subunits Cox12 and Cox13 remain in association under DDM solubilization conditions (Ref. 24 and data not shown). The level of the DDM-solubilized complex IV from wild-type or Δ*rcf1;*Δ*rcf2*+$Rcf1_{His}$ mitochondria (and also from *rcf1*$_{His}^{Q61A\ Q71A}$) was considerably greater than that observed from the Δ*rcf1;*Δ*rcf2* mitochondria, where complex IV levels (relative to the wild-type control) were reduced by ~50%, as reported previously (23). In contrast, however, the *rcf1*$_{His}^{R67A}$-containing mitochondria displayed strongly reduced levels of complex IV monomers following DDM solubilization, with levels that resembled more that of the Δ*rcf1;*Δ*rcf2* mitochondria (Fig. 2*C*). Furthermore, in addition to the monomeric complex IV population, the *rcf1*$_{His}^{R67A}$ mitochondria contained a novel complex IV subpopulation, termed IV**, that migrated slower on the BN-PAGE gel. The sum of the levels of both complex IV populations (IV + IV**) observed in the *rcf1*$_{His}^{R67A}$ mutant mitochondria following DDM solubilization were significantly lower than those from the mitochondria harboring either the $Rcf1_{His}$ or *rcf1*$_{His}^{Q61A,Q71A}$ derivatives. The reduced levels of the complex IV species (IV and IV*) observed in the DDM extracts of *rcf1*$_{His}^{R67A}$ is inconsistent with the apparently normal steady-state levels of complex IV subunits and the regular appearance of the digitonin-solubilized III-IV supercomplex in these mitochondria. Together with the observed presence of the novel complex IV** species, these results suggest that the assembly state of complex IV is altered and appears more DDM detergent-labile in *rcf1*$_{His}^{R67A}$ mitochondria compared with the wild-type control.

The presence of the novel larger IV** species in Δ*rcf1;*Δ*rcf2* mitochondria harboring the *rcf1*$_{His}^{R67A}$ derivative was unexpected, and its composition was further investigated (Fig. 3). Mitochondrial proteins were solubilized in DDM, and the complex IV populations were separated by BN-PAGE and subsequently serially analyzed by mass spectrometry. In the wild-type control, the majority of the complex IV subunits detected were present in the IV and IV* species, whereas the Cox13 pro-

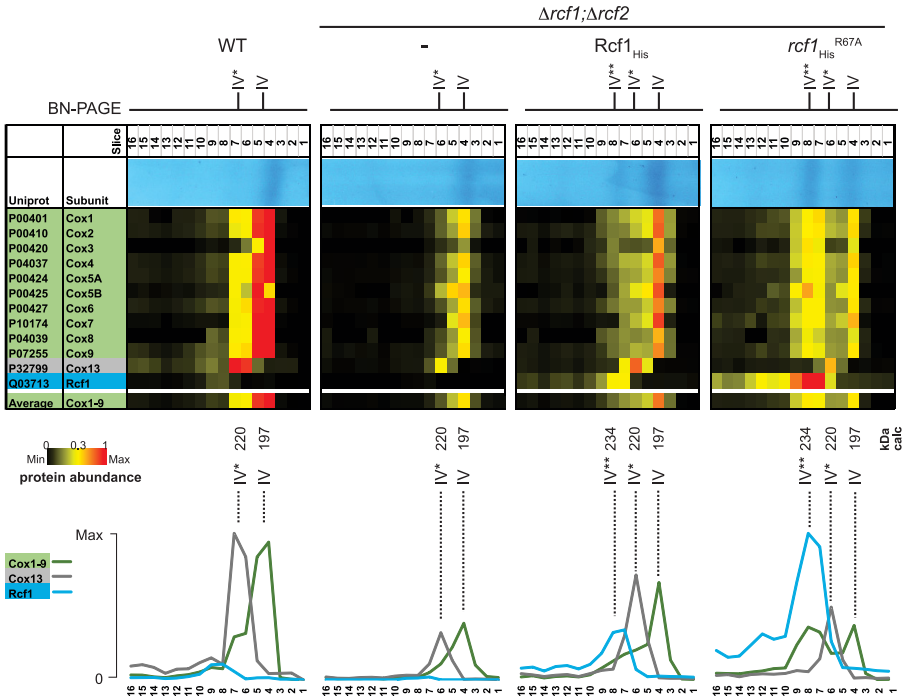

FIGURE 3. **Compositional analysis of the complex IV** subpopulation.** One-dimensional BN-PAGE analysis of protein complexes in wild-type Δ*rcf1;*Δ*rcf2* mitochondria and those harboring $Rcf1_{His}$ or $rcf1_{His}^{R67A}$ following solubilization with DDM (0.6%) was performed. The areas of the gel encompassing the complex IV and IV** species (as shown) were fractionated, and proteins were identified and quantified by mass spectrometry. The amounts of identified proteins were quantified using intensity-based absolute quantification value as described under "Experimental Procedures." Heatmaps and graphs show protein profiles normalized to the maximum abundance of a protein within BN lanes of the wild type and Δ*rcf1;*Δ*rcf2* mutants.

tein was detected only in the IV* population. (The small subunit Cox12 was not identified in the datasets.) The absence of detectable levels of Rcf1 in these complex IV or IV* populations is notable and suggests that, in the wild type, Rcf1 is not a component of the fully assembled complex IV/IV* enzyme. A small amount of Rcf1 in the wild-type sample was, however, detected in a higher molecular mass area of the BN-PAGE and co-migrated at a position of the IV** species, a species that was more evident in $rcf1_{His}^{R67A}$ mitochondria. This area of the BN gel was also populated with minor but detectable amounts of complex IV subunits, suggesting that this may correspond to a Rcf1-containing late assembly intermediate of complex IV. When the Δ*rcf1;*Δ*rcf2* mitochondria harboring the $Rcf1_{His}$ protein were analyzed, in addition to both IV and IV* populations, small but detectable levels of the IV** subpopulation and some co-migrating $Rcf1_{His}$ species were observed. However, the ratio of the IV** to the IV subpopulation was distinctly increased in $rcf1_{His}^{R67A}$ sample relative to the other mitochondrial types and in agreement with the BN-PAGE analysis shown in Fig. 2*C*. The total amount of $rcf1_{His}^{R67A}$ protein co-migrating with the IV** species was also considerably greater than that observed with the wild-type $Rcf1_{His}$ sample (also confirmed by Western blotting analysis, data not shown). Because the relative stoichiometric abundance of the complex IV subunits in the IV** species appeared similar to that of the IV species, we conclude that the novel complex IV** subpopulation is, at least in part, characterized by the stable association of the Rcf1 protein. From its mobility on the BN-PAGE, we estimated the apparent mass of IV** to be 234 kDa. The estimated mass of the IV** species (relative to the IV population, 197 kDa) would indicate that IV** may contain one copy of $Rcf1_{His}$ (19.9 kDa) with another, unknown protein of similar size or two copies of $Rcf1_{His}$. We favor that more than one copy of Rcf1 is present in the IV** subpopulation, as we have observed that the Rcf1 proteins can interact with each other and can at least form dimers (data not shown).

In summary, these findings support the conclusion that, in wild-type (or $Rcf1_{His}$) mitochondria, the majority of complex IV (*i.e.* the IV and IV* species) is not present in association with the Rcf1 protein. Furthermore, the data indicate that the $rcf1_{His}^{R67A}$ derivative may have a tighter association (possibly a higher affinity or less dynamic interaction) with complex IV than its wild-type Rcf1 counterpart and thus results in the accumulation of a larger, novel Rcf1-associated complex IV species, IV**.

The QRRQ Motif Influences the Association of Rcf1 with Complex IV and the Cox3 Subunit—The levels of complex IV associated with the His-tagged Rcf1 derivatives was next investigated through affinity purification via Ni-NTA chromatography following solubilization from mitochondria with Triton X-100 (Fig. 4*A*). A significantly higher level of complex IV subunits co-purified with the $rcf1_{His}^{R67A}$ derivative compared with the control $Rcf1_{His}$ protein analyzed in parallel (Fig. 4*A*). Consistent with the Triton X-100 lysis/purification results, enhanced association of complex IV subunits with the $rcf1_{His}^{R67A}$ derivative relative to the wild-type $Rcf1_{His}$ control was also observed under digitonin conditions (where the III-IV association is preserved) (Fig. 4*B*).

Co-purification of complex IV subunits with the $rcf1_{His}^{Q61A,Q71A}$ derivative was not observed under Triton X-100 solubilization conditions (Fig. 4*A*) but was observed (together with complex III subunits) under digitonin solubili-

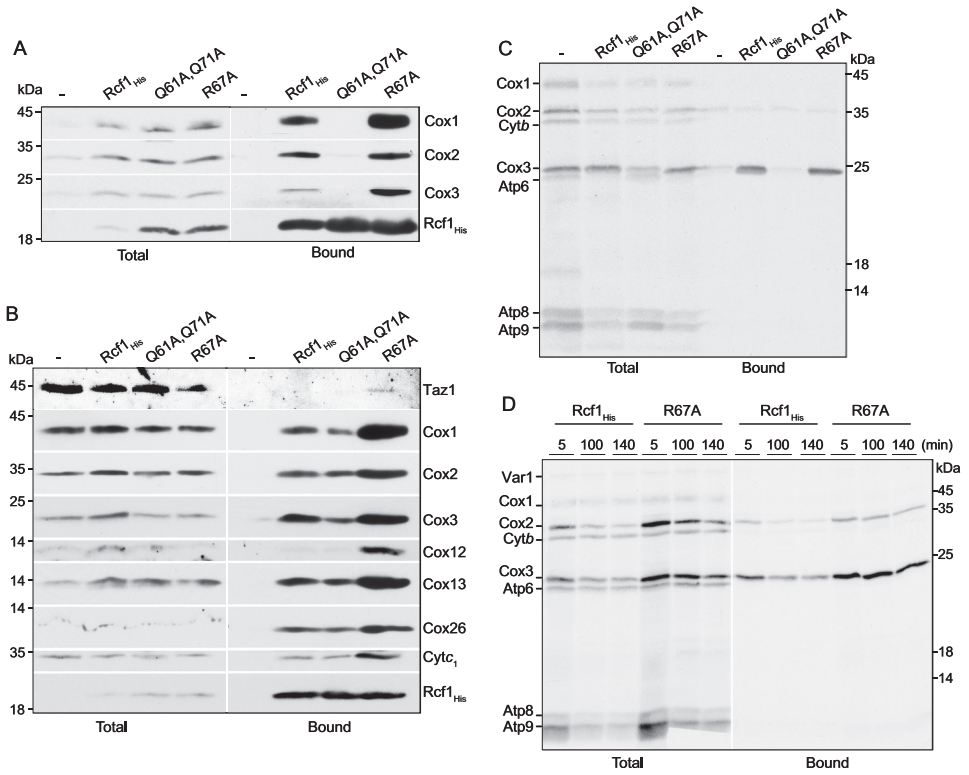

FIGURE 4. **Mutation of the QRRQ motif affects the association of Rcf1 with Cox3 and complex IV.** *A*, affinity purification of $Rcf1_{His}$, $rcf1_{His}^{Q61A,Q71A}$, $rcf1_{His}^{R67A}$ derivatives following solubilization with Triton X-100 detergent was performed, followed by SDS-PAGE, Western blotting, and immunodecoration as indicated. *Total*, 5% of solubilized material; *Bound*, 100% of affinity-purified material on the Ni-NTA beads. *B*, the same as *A*, except solubilization was performed with 1% digitonin. *C*, *in organello* labeling in the presence of [^{35}S]methionine was performed for 20 min in isolated mitochondria prior to solubilization with Triton X-100. Affinity purification of the His-tagged Rcf1 derivatives was performed as described in *A*, but, following SDS-PAGE, the gels were subjected to autoradiography. *D*, as in *C*, except, following the pulse of translation (20 min), translation was stopped through addition of puromycin and cold methionine and further chased for the time periods indicated prior to solubilization of the mitochondria with Triton X-100 and affinity purification of the Rcf1 derivatives.

zation conditions (Fig. 4*B*). Thus, mutation of the Gln^{61}/Gln^{71} residues in the QRRQ motif disturbs the integrity of the Rcf1-complex IV interaction so that it does not remain stable in the presence of Triton X-100 but can be preserved when the milder detergent (digitonin) solubilization conditions are applied. Complex IV substrate cytochrome *c* was not recovered with affinity-purified wild-type or QRRQ mutant $Rcf1_{His}$ proteins under either detergent conditions (data not shown).

Association of the Rcf1 protein with complex IV, at least in part, involves the mitochondrially encoded subunit 3, Cox3, of complex IV, which can physically associate with Rcf1 prior to its assembly into final complex IV (23). *In organello* synthesized, radiolabeled Cox3 co-purified with both wild-type $Rcf1_{His}$ and the $rcf1_{His}^{R67A}$ derivatives. Association of radiolabeled Cox3 with the $rcf1_{His}^{Q61A,Q71A}$ derivative under these Triton X-100 solubilization conditions, however, was not observed (Fig. 4*C*). Furthermore, a pulse-chase kinetic analysis indicated that the association of radiolabeled Cox3 with the $rcf1_{His}^{R67A}$ derivative appeared to be more prolonged than with the wild-type $Rcf1_{His}$ control, suggesting that mutation of the Arg^{67} residue to alanine causes enhanced association with Cox3, which may protect Cox3 from subsequent proteolytic turnover (Fig. 4*D*).

Taken together, these results indicate that mutation of the QRRQ motif has the potential to impact the nature of the Rcf1-complex IV interaction through an altered interaction with the Cox3 subunit. Mutation of Arg^{67} to alanine causes an enhanced complex IV interaction, as evidenced by the elevated levels of the complex IV** species and the increased association of complex IV subunits and radiolabeled Cox3 with the $rcf1_{His}^{R67A}$ derivative.

Complex IV in Mitochondria Harboring the $rcf1_{His}^{R67A}$ Derivative Displays Altered Enzymatic Properties—The enzymatic properties of complex IV in $rcf1_{His}^{R67A}$ mitochondria were explored next. The complex IV enzyme solubilized in DDM retains its enzymatic activity, as evidenced by "in-gel" activity assays performed with exogenously added cytochrome *c* and diaminobenzidine following BN-PAGE analysis (Fig. 5*A*, *center panel*). The level of complex IV activity was strongly reduced in the Δ*rcf1;*Δ*rcf2* mutant compared with both the wild-type control and the null mutant harboring the $Rcf1_{His}$ protein. This reduced complex IV enzyme activity can be attributed to the reduction in complex IV protein levels in the Δ*rcf1;*Δ*rcf2* mutant (Figs. 2*C* and 5*A*). Despite also having reduced protein content (as judged by parallel Western blotting analysis; Fig. 5*A*, *top panel*), the levels of DDM-solubilized complex IV enzyme activity in both the IV and IV** subpopulations in the $rcf1_{His}^{R67A}$ sample appeared similar to, or even higher than, those obtained for the IV population in the Δ*rcf1;* Δ*rcf2*+$Rcf1_{His}$ or the $rcf1_{His}^{Q61A,Q71A}$ mitochondria (Fig. 5*A*, *center panel*). These results suggest that the complex IV/IV** subpopulations solubilized from $rcf1_{His}^{R67A}$ exhibit an increased level of enzyme-specific activity.

The O_2 consumption capacity of mitochondria harboring the Rcf1 derivatives under different bioenergetic states was mea-

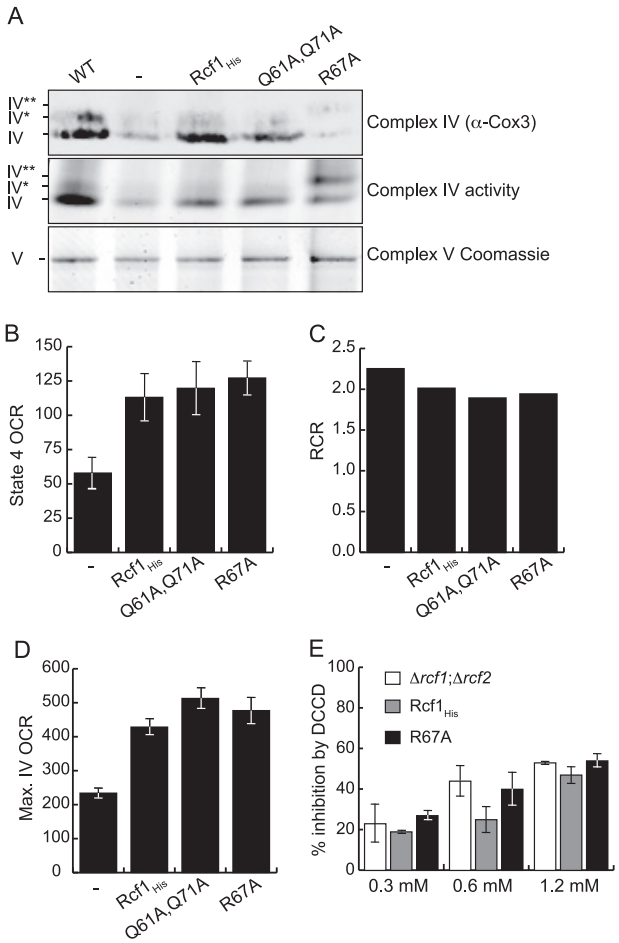

FIGURE 5. **Complex IV in $rcf1_{His}^{R67A}$ mitochondria displays altered catalytic properties.** *A*, mitochondria isolated from WT or the Δ*rcf1*;Δ*rcf2* strain harboring the $Rcf1_{His}$, $rcf1_{His}^{Q61A,Q71A}$, $rcf1_{His}^{R67A}$ derivatives, as indicated, were solubilized with DDM (0.6%) and subjected to duplicate BN-PAGE analysis. The complex IV enzyme activity levels were analyzed in one set of samples by performing an in-gel enzyme assay (*center panel*), and in a parallel sample, the complex IV protein levels were determining following Western blotting and decoration with Cox3 antibody (*top panel*), as indicated. The levels of Coomassie-stained complex V (F_1F_0-ATP synthase) are shown in the *bottom panel* as a loading control. *B* and *C*, the OCRs of the NADH-driven state 4 and respiratory control ratio (the ratio of state 3 (NADH/ADP) to state 4 (NADH)) were measured in the indicated isolated mitochondria ($n = 3$). *D*, the maximal capacity of complex IV was determined by measuring the OCR driven by ascorbate/TMPD in the presence of CCCP to dissipate the membrane potential ($n = 6$). *E*, isolated Δ*rcf1*;Δ*rcf2* mitochondria and Δ*rcf1*;Δ*rcf2* harboring the $Rcf1_{His}$ or $rcf1_{His}^{R67A}$ derivatives were incubated with DCCD at the indicated concentrations for 90 min at room temperature prior to measuring the maximal complex IV OCR in the presence of ascorbate/TMPD and CCCP. The percent of inhibition caused by the DCCD treatment relative to the control (no DCCD) is indicated.

sured. The rates of O_2 consumption following addition of the substrate NADH, *i.e.* basal or "state 4" respiration, were similar in all mitochondrial types, *i.e.* harboring either the $Rcf1_{His}$, $rcf1_{His}^{Q61A,Q71A}$ or $rcf1_{His}^{R67A}$ proteins. The respiratory control rate (state 3 respiration [NADH+ADP]/state 4) in QRRQ mutant mitochondria was also similar to the other mitochondria measured, indicating the coupled state of these mitochondria (Fig. 5*C*). The maximum oxygen consumption capacity of complex IV (measured in the presence of ascorbate/TMPD/CCCP) was also found to be similar in mitochondria harboring both wild-type $Rcf1_{His}$ and the QRRQ mutant derivatives (Fig. 5*D*). Therefore, we conclude that both the $rcf1_{His}^{Q61A,Q71A}$ and $rcf1_{His}^{R67A}$ mutant derivatives displayed the capacity to fully support maximal complex IV activity when expressed in the Δ*rcf1*;Δ*rcf2* strain even when the enzyme is working to its maximum capacity.

Finally, the observed elevated in-gel enzyme activity assay suggests that the complex IV enzyme in the $rcf1_{His}^{R67A}$ mitochondria may display differential enzymatic properties than when the wild-type Rcf1 control protein is present. In support of this, we also observed that the complex IV enzyme in $rcf1_{His}^{R67A}$ mitochondria displayed an increased sensitivity to DCCD relative to those harboring the wild-type $Rcf1_{His}$ (Fig. 5*E*). A similar effect was observed in Δ*rcf1*;Δ*rcf2* mitochondria. DCCD binds to Cox3 (Glu^{90} residue in bovine Cox3, equivalent to Glu^{98} in yeast) and, in doing so, interferes with the oxygen uptake pathway of complex IV, which involves associated lipids, phosphatidylglycerol (PG1/PG2), and CL molecules within the enzyme (29, 30). We speculate that structural changes in complex IV in $rcf1_{His}^{R67A}$ mitochondria may alter the accessibility of DCCD to its target. Alterations in the lipid composition of complex IV may underlie this and would be consistent with the observed instability of complex IV from $rcf1_{His}^{R67A}$ mitochondria to extraction with the detergent DDM.

Rcf1 May Be Involved in Posttranslational Modification of Complex IV—Analysis of the amino acid sequence region encompassing the QRRQ motif in an α-helical plot indicated that the Arg^{67} residue co-aligned with the Gln^{71} residue, where the Gln^{61} residue neighbored the Arg^{65} residue, suggesting that they may form Gln/Arg pairs (Fig. 6*A*). We further explored the QRRQ motif in the Rcf1 protein by making double mutants, mutating one or other of the Gln/Arg pairs, *i.e.* $rcf1_{His}^{Q61A,R65A}$ and $rcf1_{His}^{R67A,Q71A}$, and then expressed them in the Δ*rcf1*;Δ*rcf2* null mutant. Steady-state analysis of proteins isolated from the resulting strains indicated that the levels of both mutant Rcf1 derivatives were strongly reduced, in particular the $rcf1_{His}^{Q61A,R65A}$ derivative, compared with the wild-type $Rcf1_{His}$ control (Fig. 6*B*). Thus, mutation of either of the Gln/Arg pairs in this manner strongly impacted the stability and steady-state levels of the Rcf1 protein. Mutation of residue Arg^{65} alone (*i.e.* $rcf1_{His}^{R65A}$) did not compromise the stability of Rcf1 or its ability to support the assembly of a functional complex IV (supplemental Fig. S1). Similar to the $rcf1_{His}^{R67A}$ derivative (albeit to a lesser extent), an increase in the level of complex III-IV subunits in association with the affinity-purified $rcf1_{His}^{R65A}$ derivative was observed (supplemental Fig. S1).

Despite the strongly reduced levels of the $rcf1_{His}^{Q61A,R65A}$ protein, the complex IV subunit levels in the mutant mitochondria were similar to that of the $Rcf1_{His}$ control and significantly higher than those observed in the Δ*rcf1*;Δ*rcf2* null mitochondria (Fig. 6*B*). The organization and levels of the III-IV supercomplex in the $rcf1_{His}^{Q61A,R65A}$ mitochondria also resembled those of the $Rcf1_{His}$ control analyzed in parallel (Fig. 6*C*, *top panel*). Furthermore, the levels of DDM-solubilized complex IV in the $rcf1_{His}^{Q61A,R65A}$ mitochondria were similar to those of the wild-type $Rcf1_{His}$ control (Fig. 6*C*, *bottom panel*).

Although the steady-state levels of the $rcf1_{His}^{R67A,Q71A}$ derivative were marginally higher than that of $rcf1_{His}^{Q61A,R65A}$ protein, the presence of the $rcf1_{His}^{R67A,Q71A}$ protein only partially restored the complex IV subunits to wild-type levels, indicating

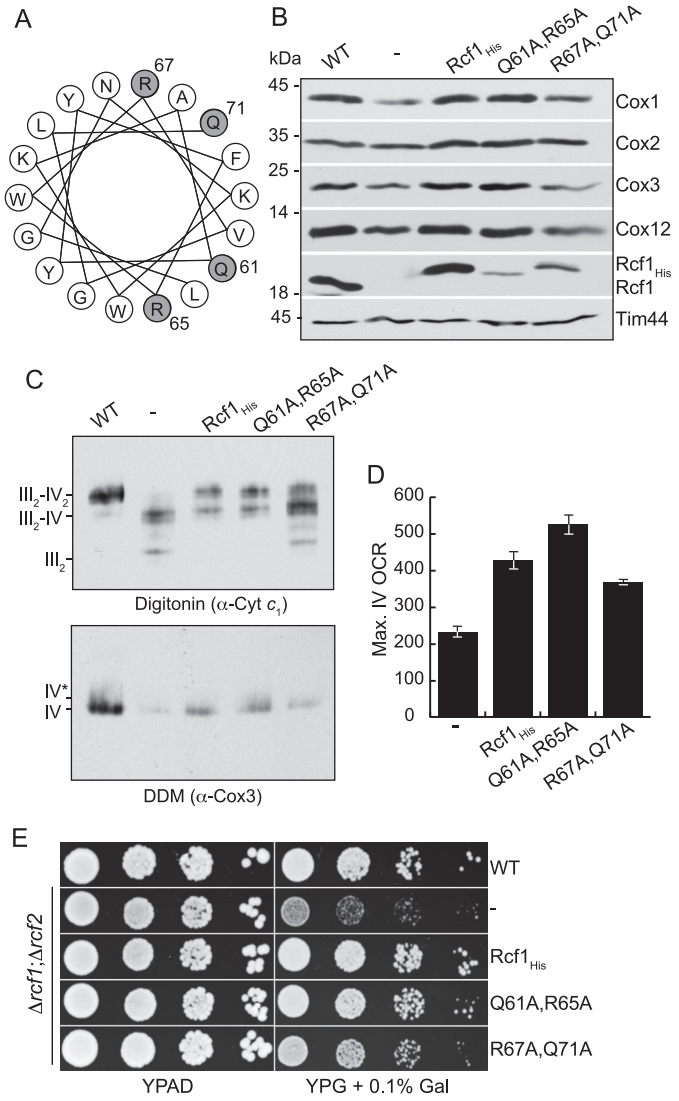

FIGURE 6. **Mutation of the Glu/Arg pairs in the QRRQ motif in Rcf1 affects the stability of Rcf1, but complex IV assembles.** *A*, an α-helical plot of residues Leu^{54} through Gln^{71} of Rcf1 depicting the co-localization of the Gln^{61}/Arg^{65} residue pair and the Arg^{67}/Gln^{71} residue pair on the helix. *B*, steady-state levels of the OXPHOS subunits in the mitochondria (50 μg of protein) isolated from the indicated strains. Tim44 was used as a loading control. *C*, mitochondria isolated from the WT and the indicated Δ*rcf1*,Δ*rcf2* strains were solubilized in digitonin (1%, *top panel*) or DDM (0.6%, *bottom panel*) and subjected to BN-PAGE analysis, Western blotting, and immunodecoration with antibodies against the complex III subunit, cytochrome c_1 (α-*Cytc*$_1$, *top panel*) and the complex IV subunit, Cox3 (*bottom panel*). *D*, maximal OCR of bioenergetically isolated complex IV was measured in mitochondria isolated from the Δ*rcf1*;Δ*rcf2* strain and the Δ*rcf1*;Δ*rcf2* strain harboring the *rcf1*$_{His}^{Q61A,R65A}$ or *rcf1*$_{His}^{R67A,Q71A}$ derivatives following addition of ascorbate/TMPD and CCCP. *E*, serial 10-fold dilutions of WT, and Δ*rcf1*;Δ*rcf2* expressing Rcf1$_{His}$, *rcf1*$_{His}^{Q61A,R65A}$, *rcf1*$_{His}^{R67A,Q71A}$ derivatives or not, as indicated, were spotted on YP plates containing glucose (*YPAD*) or glycerol supplemented with 0.1% galactose (*YPG + 0.1% Gal*) and grown at 30 °C.

that the ability of this Rcf1 derivative to support complex IV assembly was compromised through mutation of the Arg^{67}/Gln^{71} pair (Fig. 6*B*). Consistently, a partial restoration of the III_2-IV_{1-2} species was observed in the BN-PAGE analysis of the digitonin-solubilized *rcf1*$_{His}^{R67A,Q71A}$ mitochondria, paralleling the observation that the levels of the complex IV subunits in these mitochondria were greater than those in the Δ*rcf1*;Δ*rcf2* control but not equivalent to those of the wild-type control (or of the *rcf1*$_{His}^{Q61A,R65A}$ mitochondria) (Fig. 6*C*, *top panel*). However, when solubilized with DDM, the levels of free complex IV from *rcf1*$_{His}^{R67A,Q71A}$ mitochondria appeared similar to those of the Δ*rcf1*;Δ*rcf2* null mitochondria and in contrast to those from the *rcf1*$_{His}^{Q61A,R65A}$ mitochondria, where the levels of complex IV were similar to the wild-type Rcf1$_{His}$ control (Fig. 6*C*, *bottom panel*). These results together suggest that complex IV from the *rcf1*$_{His}^{R67A,Q71A}$ mitochondria may exhibit some detergent instability to DDM extraction in a similar manner as observed previously in the *rcf1*$_{His}^{R67A}$ mitochondria (Fig. 3*C*). In contrast to the *rcf1*$_{His}^{R67A}$ mitochondria, the presence of a complex IV** form was not detected in the *rcf1*$_{His}^{R67A,Q71A}$ mitochondrial sample. This may be attributed to the strongly reduced of levels of *rcf1*$_{His}^{R67A,Q71A}$ derivative in these mitochondria and, thus, would be limiting to form detectable levels of the complex IV** species, and/or the introduction of the additional Q71A mutation may have compromised the stability of the Rcf1-complex IV association.

Measurement of the maximal O_2 consumption rates of complex IV in the *rcf1*$_{His}^{Q61A,R65A}$ mitochondria demonstrated them to be fully restored to the levels in wild-type Rcf1$_{His}$ control mitochondria, whereas, in *rcf1*$_{His}^{R67A,Q71A}$ mitochondria, although they were significantly higher than those measured in the Δ*rcf1*;Δ*rcf2* null mitochondria, they were not equivalent to the *rcf1*$_{His}^{Q61A,R65A}$ or wild-type Rcf1$_{His}$ mitochondria (Fig. 6*D*). The increased level of complex IV activity in both of these mutants was sufficient to restore aerobic growth, as expression of both *rcf1*$_{His}^{Q61A,R65A}$ and *rcf1*$_{His}^{R67A,Q71A}$ derivatives ensured complementation of the growth defect phenotype of the Δ*rcf1*;Δ*rcf2* strain (Fig. 6*E*).

In summary, the Gln^{61}/Arg^{65} and Arg^{67}/Gln^{71} residue pairs within the QRRQ motif of Rcf1 are independently critical for the stability of the Rcf1 protein. However, despite being strongly reduced in levels, the Gln/Arg pair mutated Rcf1 derivatives could support (fully for the Gln^{61}/Arg^{65} mutant and partially for the Arg^{67}/Gln^{71} mutant) the assembly and activity of complex IV.

The Integrity of the Rcf1 QRRQ Motif Alters the Molecular Environment of the Rcf1 Protein—As described previously, wild-type Rcf1$_{His}$ forms a number of adducts with the cross-linking reagent MBS, the most notable being a 45-kDa adduct reported previously to represent cross-linking of Rcf1 to the AAC proteins (23). The *rcf1*$_{His}^{Q61A,Q71A}$ derivative maintained the ability to be cross-linked to AAC, whereas the cross-linking between *rcf1*$_{His}^{R67A}$ and AAC was significantly reduced (Fig. 7*A*) despite the normal levels of the AAC protein in these mitochondria (Fig. 2*C*). The MBS cross-linking profile of the *rcf1*$_{His}^{R65A}$ derivative resembled that of the *rcf1*$_{His}^{R67A}$ protein (supplemental Fig. S1). In addition to the loss of the Rcf1-AAC adduct in *rcf1*$_{His}^{R67A}$ mitochondria, we observed the gain of a novel adduct near 50 kDa. This *rcf1*$_{His}^{R67A}$ adduct was close in size to, but distinct from, a 52-kDa Rcf1 adduct observed in Rcf1$_{His}$ and *rcf1*$_{His}^{Q61A,Q71A}$ mitochondria. As the mass of the 50-kDa Rcf1 adduct was similar to the sum of the His-tagged Rcf1 (20 kDa) and subunit 2 of complex IV, Cox2 (30 kDa), we explored whether this represented an Rcf1-Cox2 adduct. Decoration of a parallel experiment with Cox2-specific-antiserum demonstrated that a MBS-formed adduct of similar size (~50

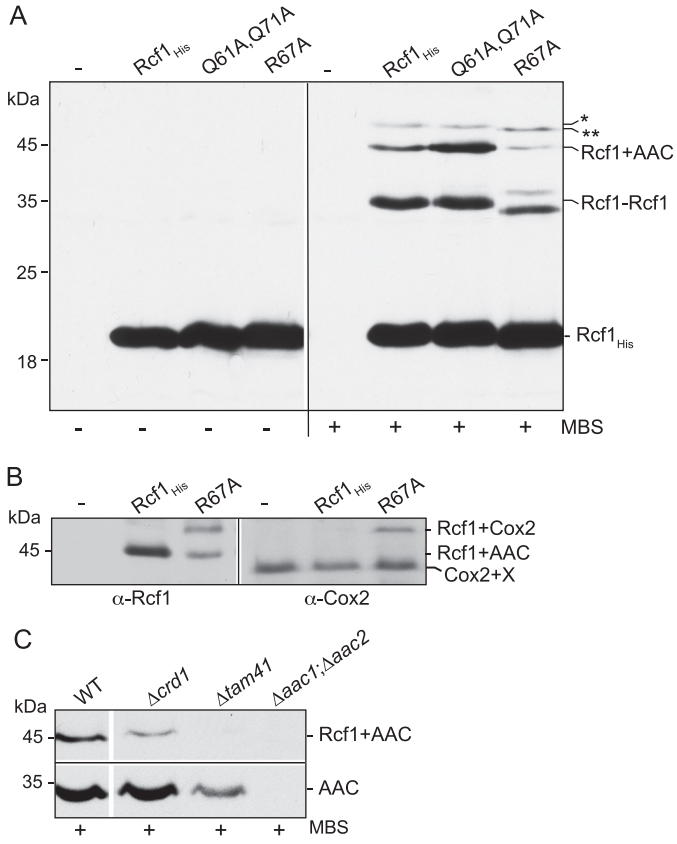

FIGURE 7. **Mutation of the QRRQ motif or the absence of CL alters the environment of Rcf1.** *A*, chemical cross-linking using MBS was performed on mitochondria isolated from the Δ*rcf1;*Δ*rcf2* strain harboring either the wild-type $Rcf1_{His}$, $rcf1_{His}^{Q61A,Q71A}$, or $rcf1_{His}^{R67A}$ mutant derivatives as indicated. Following SDS-PAGE and Western blotting, decoration with His tag epitope antiserum was performed. The positions of the dominant 45-kDa (*Rcf1-AAC*) and 36-kDa (*Rcf1-Rcf1*) Rcf1-containing adducts are indicated. The position of a less abundant Rcf1 50-kDa adduct detected in $rcf1_{His}^{R67A}$ mitochondria is indicated by *two asterisks*. Note that a slightly larger (52-kDa), still uncharacterized Rcf1 adduct is also observed in the $Rcf1_{His}$ or $rcf1_{His}^{Q61A,Q71A}$ mitochondria and is indicated by *one asterisk*. *B*, cross-linking was performed and analyzed as described in *A*. Parallel Western blots were decorated with either Rcf1 (*left panel*) or Cox2 (*right panel*) antiserum. Only the area encompassing the 50-kDa Rcf1-Cox2 adduct is shown. *C*, cross-linking of Rcf1 was performed in mitochondria isolated from the wild type, Δ*crd1*, Δ*tam41*, and Δ*aac2*,Δ*aac1* strains, as indicated. Samples were further analyzed as described in *A* using Rcf1 (*top panel*) or AAC-specific (*bottom panel*) antibodies. Only the areas of the gel encompassing both the 45-kDa Rcf1-AAC adduct and the monomeric AAC are shown.

kDa) was detected with both Rcf1 and Cox2 antisera in Δ*rcf1;* Δ*rcf2* mitochondria harboring the $rcf1_{His}^{R67A}$ mutant derivative (Fig. 7*B*). In contrast, no Cox2-containing adduct was detected in Δ*rcf1;*Δ*rcf2* mitochondria harboring His-tagged wild-type Rcf1 or the $rcf1_{His}^{Q61A,Q71A}$ derivative (data not shown) and consistent with the Rcf1-antibody decoration. We therefore conclude that the arrangement of Rcf1 with complex IV is altered in the $rcf1_{His}^{R67A}$ mutant so that a close proximity between Rcf1 and Cox2 is gained and revealed through the cross-linking approach.

Similar to the $rcf1_{His}^{R67A}$ mitochondria, loss of Rcf1-AAC adduct formation was also observed in mitochondria isolated from mutants displaying defective CL biosynthesis, such as the CL synthase mutant Δ*crd1* (where AAC levels are normal) or the Tam41 null mutant Δ*tam41* (Fig. 7*C*) (albeit with reduced levels of AAC). Tam41 is a CDP-diacylglycerol synthase required for CL biosynthesis in mitochondria, and thus, like the Δ*crd1*, Δ*tam41* mitochondria are deficient in CL (31). Interestingly, despite being reduced in levels, a population of Taz1, an enzyme involved in remodeling of CL, was recovered in association with the affinity-purified $rcf1_{His}^{R67A}$ protein (Fig. 4*B*). Taz1 has also been found previously in association with the CL-containing AAC protein (32). Taken together, these results indicate that the molecular environment of Rcf1 is altered through the R67A (and R65A) mutation and in a similar manner as that observed for wild-type Rcf1 in mitochondria deficient in CL.

Discussion

Here we have studied the yeast Hig1 protein Rcf1, a member of the Hig1 type 2 subgroup, and have probed the functional importance of the conserved QRRQ motif of Rcf1, an important distinguishing feature between the type 2 and type 1 subgroups of the Hig1 protein family. Our findings here indicate that the QRRQ motif may form Gln/Arg pairs (Gln^{61}/Arg^{65} and Arg^{67}/Gln^{71}), which serve to support the stability of the Rcf1 protein within the mitochondrial membrane. Furthermore, our data demonstrate that an intact QRRQ motif supports the ability of Rcf1 to associate with complex IV, in particular with Cox3 and Cox2 subunits, and facilitate the correct maturation and stable assembly of the complex IV enzyme. In particular, our results illustrate the importance of the residue Arg^{67} in modulating the interaction of Rcf1 with Cox3/complex IV.

How do Rcf1 and the Hig1 family members support complex IV assembly/activity and how is this related to their QRRQ motif? One possibility is that Rcf1 represents a physical component (*i.e.* a stoichiometric subunit) of complex IV and, through Cox3 (and possibly Cox2), may serve to enhance the structure and activity of this enzyme in a manner that influences the association of both Cox12 and the substrate cytochrome *c* (23). Thus, by binding as an additional subunit to subpopulations of the enzyme (*i.e.* in stoichiometrically equivalent amounts as other complex IV subunits), Rcf1 may exert an influence over substrate binding and the enzymatic properties of complex IV. Indeed, the binding of a Hig1 family member, HIGD1A, to the complex IV enzyme has been indicated to enhance the activity of the enzyme (33), and evidence to indicate altered cytochrome *c* binding properties to the complex IV enzyme is obtained in mitochondria lacking the Rcf1 protein (15).

On the other hand, it was suggested previously that Rcf1 may play a role in the proper assembly of complex IV rather than acting as a stoichiometric component supporting the III-IV supercomplex arrangement (34). A number of lines of evidence presented here support this proposal. First, the BN-PAGE/proteomic analysis demonstrates that $Rcf1/Rcf1_{His}$ is not found in association with the predominant subpopulations of complex IV, *i.e.* the IV/IV* species, and is recovered only with the IV** subpopulation. The IV** species represented a minor population of total complex IV in wild-type (or in Δ*rcf1*; Δ*rcf2*+$Rcf1_{His}$) mitochondria, and the level of IV** was significantly increased through the R67A mutation, which also promoted the Rcf1-Cox3 interaction. Consistently, earlier

BN-PAGE and affinity purification approaches have shown that the majority of Rcf1 is not together with complex IV, and only a minor percentage of complex IV is recovered together with Rcf1 (23). Second, an enhanced specific activity of both complex IV and the novel IV** species was observed through in-gel complex IV activity analysis in the extracts of the $rcf1_{His}^{R67A}$ mitochondria, yet the $rcf1_{His}^{R67A}$ protein was present in association with only the IV** species. Third, complex IV activity (and steady-state levels) were fully restored in the Δ*rcf1*;Δ*rcf2* mutant harboring the $rcf1_{His}^{Q61A,R65A}$ protein (and partially in those containing the $rcf1_{His}^{R67A,Q71A}$ protein) despite the strongly reduced levels of these mutated Rcf1 derivatives. These findings indicate that Rcf1 does not need to be present at its wild-type levels to fully support the activity of complex IV and, thus, argue against Rcf1 exerting its influence on complex IV activity as a stoichiometric equivalent component of the enzyme.

Taking these findings together, we propose here that Rcf1 functions to support the assembly and activity of complex IV by dynamic and transient associations with it, possibly during the assembly process to modify the enzyme composition and, thereby, its stability and catalytic properties. Thus, when analyzed, only a small fraction of complex IV is found in association with Rcf1, and this may reflect a late-stage Rcf1-complex IV assembly intermediate or a small population of the assembled complex IV being modified in an Rcf1-dependent fashion. Moreover, we suggest that this modification of complex IV, *i.e.* Rcf1's "fingerprint" on it, may involve non-protein elements of complex IV, such as associated lipids. The association of Rcf1 with Cox3-containing assembly intermediates may be important to secure the correct maturation (or regulatory modification) of this subunit. We speculate that an otherwise transient interaction of Rcf1 and Cox3 protein is stalled upon mutation of the key Arg^{67} residue, and thus, more of complex IV (IV**) remains in association with the $rcf1_{His}^{R67A}$ species, and this may have interfered with the normal maturation and stability of the enzyme. A number of results reported here support the speculation that the function of the fingerprint of Rcf1 may be related to the incorporation or remodeling of the CL or other lipid species associated with the complex IV enzyme. Both CL and PG lipids are associated with complex IV, in particular with the Cox3 subunit, and together are proposed to form an integral part of the O_2 translocation channel to the active site of the enzyme (30). The observed instability of the complex IV enzyme to DDM detergent extraction and the increased sensitivity to DCCD inhibition in $rcf1_{His}^{R67A}$ mitochondria may suggest an altered CL and/or PG arrangement within the complex IV enzyme.

A possible role for Rcf1 in the lipid maturation of mitochondrial enzyme complexes may not be limited to complex IV, as we also demonstrate that the $rcf1_{His}^{R67A}$ mutant displays a decreased ability to cross-link to AAC proteins, a result that was mirrored with the wild-type Rcf1 protein in the CL-deficient mitochondria Δ*crd1* and Δ*tam41*. Rcf1 has been shown to exist in a close physical relationship with the Cox3, Cox12, AAC proteins (Ref. 23 and our results here), and also with cytochrome c_1 of complex III (22),[3] and all are proteins known to be intimately associated with CL molecules. Lipid profile analysis of Δ*rcf1*;Δ*rcf2* mutant mitochondria has not indicated a major alteration in the content of CL or PG in the absence of Rcf1/Rcf2 proteins.[4] The recovery of a population of Taz1 with the $rcf1_{His}^{R67A}$ mutant may also add further support to a possible involvement of Rcf1 in CL maturation or remodeling within the mitochondrial membrane complexes.

Finally, as our data highlight the importance of the QRRQ motif for the function of Rcf1, a Hig1 type 2 family member, it is important to note that this motif is noticeably different in the Hig1 type 1, stress-induced isoforms, where the QRRQ motif is replaced with (I/V/L)HLIHMRX_3Q. It is possible that the differences in these motifs between the type 2 and type 1 Hig1 family members reflect the need for differential lipid modifications of complex IV and other enzymes, designed to fine-tune the respiratory chain to operate under stress conditions such as hypoxia.

Experimental Procedures

Yeast Strains and Growth Conditions—All *S. cerevisiae* strains used in this study were in the haploid W303–1A genetic background (W303-1A, *mat* a *leu2, trp1, ura3, his3, ade2*) and include the WT, Δ*rcf1*;Δ*rcf2* (*RCF1:: HIS3, RCF2::KAN*) (23), Δ*aac2* (*AAC2::KAN*) (35), Δ*tam41* (MMP37::*KAN*) (36), and Δ*crd1* (*CRD1::KAN*). Yeast strains were maintained and cultured at 30 °C on YP (yeast extract, peptone) medium supplemented with 2% glucose and 20 mg/liter adenine hemisulfate (YPAD) following standard protocols. All cultures were grown in YP medium containing 0.5% lactate and supplemented with 2% galactose.

Generation of His-tagged Rcf1 QRRQ Mutant Derivatives—The Yip351-LEU2 vector containing the open reading frame encoding the Rcf1 protein as a C-terminal His_{12}-tagged protein downstream of the galactose-inducible GAL10 promoter (23) was used as a template for PCR-based mutagenesis. Mutations in the QRRQ motif were generated using a PCR site-directed mutagenesis strategy. The resulting plasmids were integrated into the *leu2* locus of the Δ*rcf1*;Δ*rcf2* strain, LEU^+ transformants were selected, and expression of $Rcf1_{His}$ derivatives was verified.

Affinity Purification of His-tagged Proteins—Isolated mitochondria (200 μg of protein) harboring the His-tagged Rcf1 derivatives were solubilized in lysis buffer (100 mM KCl, 20 mM HEPES-KOH, 10 mM $MgCl_2$, and 0.5 mM PMSF (pH 7.4)) containing either 0.25% Triton X-100, 0.6% DDM, or 1% digitonin (as indicated) for 30 min on ice. Following a clarifying spin, Ni-NTA purification of His-tagged proteins was performed as described previously (37).

BN-PAGE Analysis—BN-PAGE analysis of digitonin-solubilized (1%) or DDM-solubilized (0.6%) mitochondrial extracts (30 μg of protein) was performed using Invitrogen NuPAGE gradient (4–12%) gels according to the protocol of the manufacturer, followed by Western blotting and immunodecoration with subunit-specific antisera as indicated. For in-gel complex

[3] J. Garlich and R. A. Stuart, unpublished results.
[4] S. Claypool, personal communication.

IV activity following BN-PAGE (0.6% DDM lysis), the gel was incubated in activity buffer (50 mM phosphate buffer (pH 7.4), 1 mg/ml 3,3′ diaminobenzidine, 1 nM catalase, 1 mg/ml cytochrome *c*, and 75 mg/ml sucrose) for 90 min at room temperature, fixed for 1 h in 45% methanol and 10% acetic acid, and destained overnight in 10% methanol and 10% acetic acid.

Quantitative Mass Spectrometry—Protein abundance profiles of subunits within complexes were analyzed by a combination of BN-PAGE and quantitative MS (38). Briefly, the area of the complex IV species in the BN-PAGE gel (linear 3–18% acrylamide gradient) was cut into 16 even slices, digested with trypsin as described previously (38), and further analyzed as described previously (28). MS data were analyzed by MaxQuant (v1.5.3.30) (39). Proteins were identified using the yeast reference proteome database UniProtKB with 6721 entries, released in March 2016, supplemented with the Rcf1-His derivatives as described previously (28). Intensity-based absolute quantification values were recorded and normalized to maximum appearance within native lanes comparing wild-type, Δ*rcf1;*Δ*rcf2,* Δ*rcf1;*Δ*rcf2*+$Rcf1_{His}$, and Δ*rcf1;*Δ*rcf2*+$rcf1_{His}^{R67A}$. To compare these mini abundance profiles, each sample was normalized to the median of protein abundance of the wild type (28). Normalization to the maximum appearance of each protein within the analyzed samples was used to display the results in heatmaps and profile plots. Complexes III_2 (473 kDa), ATP synthase (572 kDa), IV (sum of all matured subunits, two copies of Cox8, without Cox12 and Cox13, 197 kDa) were used for native mass calibration (data not shown).

O_2 Consumption Assays—Oxygen consumption rates (OCRs) were measured with a Clark-type oxygen electrode (Rank Brothers, digital model 10) using isolated mitochondria (80 μg of protein) in an isosmotic buffer (10 mM potassium P_i, 20 mM HEPES-KOH, 2 mM $MgCl_2$, 1 mM EDTA, 1 mg/ml BSA, and 0.6 M mannitol (pH 7.2)). State 4 respiration was measured following addition of NADH (0.5 mM), and state 3 was then achieved by subsequent addition of ADP (0.2 mM). The bioenergetically isolated complex IV OCR was attained by addition of TMPD/ascorbate (0.4 mM/1.6 mM) to directly reduce cytochrome *c*, and maximal bioenergetically isolated complex IV activity was achieved by subsequent addition of a protonophore (CCCP, 0.2 mM). DCCD inhibition of bioenergetically isolated complex IV was measured as above following 90-min, 25 °C incubation of mitochondria in MES-Tris buffer (pH 7.3) containing 10% methanol and 0.3, 0.6, or 1.2 mM DCCD (in methanol) or control (methanol alone).

Miscellaneous—In organello translation with [^{35}S]methionine labeling was performed as described previously (40). Chemical cross-linking with *m*-maleimidobenzoyl-*N*-hydroxysuccinimide ester (MBS) was performed as described previously (23). Mitochondrial isolation, protein determination, and SDS-PAGE were performed according to published methods (21, 41, 42). The Cox1 and Cox3 antibodies used in this study were commercially obtained (Cox1: Molecular Probes, anti-yeast Cox1, mouse monoclonal 11D8-B7, lot 6251–1; Cox3: Invitrogen/Novex anti-Cox3 monoclonal, 459300, lot H3578). All other antibodies used were rabbit polyclonal against the respective purified yeast proteins and generated either in the Stuart laboratory or received as gifts.

Author Contributions—J. G. and R. A. S. conceived and coordinated the study and wrote the paper. J. G. designed, performed, and analyzed all the experiments shown together with R. A. S., except those shown in Fig. 3. V. S. and I. W. performed and analyzed the experiments shown in Fig. 3 and prepared the figure. J. G. prepared all other figures. All authors reviewed the results and approved the final version of the manuscript.

Acknowledgments—We thank Vera Strogolova, Jodie Box, and Jonathan Scheel for contributions to this project. We also thank Dr. Klaus Pfanner (Freiburg, Germany) for the valuable gift of complex IV subunit (Cox6 and Cox12) antisera and Dr. Steve Claypool (Johns Hopkins University School of Medicine) for the Taz1 antiserum.

References

1. Schägger, H. (2002) Respiratory chain supercomplexes of mitochondria and bacteria. *BBA - Bioenergetics* **1555,** 154–159
2. Stuart, R. A. (2008) Supercomplex organization of the oxidative phosphorylation enzymes in yeast mitochondria. *J. Bioenerg. Biomembr.* **40,** 411–417
3. Lenaz, G., and Genova, M. L. (2009) Structural and functional organization of the mitochondrial respiratory chain: a dynamic super-assembly. *Int. J. Biochem. Cell Biol.* **41,** 1750–1772
4. Nunnari, J., and Suomalainen, A. (2012) Mitochondria: in sickness and in health. *Cell* **148,** 1145–1159
5. Tsukihara, T., Aoyama, H., Yamashita, E., Tomizaki, T., Yamaguchi, H., Shinzawa-Itoh, K., Nakashima, R., Yaono, R., and Yoshikawa, S. (1996) The whole structure of the 13-subunit oxidized cytochrome *c* oxidase at 2.8 Å. *Science* **272,** 1136–1144
6. Fontanesi, F., Soto, I. C., and Barrientos, A. (2008) Cytochrome *c* oxidase biogenesis: new levels of regulation. *IUBMB Life* **60,** 557–568
7. Mick, D. U., Fox, T. D., and Rehling, P. (2011) Inventory control: cytochrome *c* oxidase assembly regulates mitochondrial translation. *Nat. Rev. Mol. Cell Biol.* **12,** 14–20
8. Saraste, M. (1999) Oxidative phosphorylation at the fin de siècle. *Science* **283,** 1488–1493
9. Pebay-Peyroula, E., and Brandolin, G. (2004) Nucleotide exchange in mitochondria: insight at a molecular level. *Curr. Opin. Struct. Biol.* **14,** 420–425
10. Cruciat, C. M., Brunner, S., Baumann, F., Neupert, W., and Stuart, R. A. (2000) The cytochrome bc_1 and cytochrome *c* oxidase complexes associate to form a single supracomplex in yeast mitochondria. *J. Biol. Chem.* **275,** 18093–18098
11. Heinemeyer, J., Braun, H. P., Boekema, E. J., and Kouril, R. (2007) A Structural model of the cytochrome *c* reductase/oxidase supercomplex from yeast mitochondria. *J. Biol. Chem.* **282,** 12240–12248
12. Claypool, S. M., Oktay, Y., Boontheung, P., Loo, J. A., and Koehler, C. M. (2008) Cardiolipin defines the interactome of the major ADP/ATP carrier protein of the mitochondrial inner membrane. *J. Cell Biol.* **182,** 937–950
13. Stuart, R. A. (2009) Chapter 11 supercomplex organization of the yeast respiratory chain complexes and the ADP/ATP carrier proteins. *Methods Enzymol.* **456,** 191–208
14. Dudkina, N. V., Kouril, R., Peters, K., Braun, H.-P., and Boekema, E. J. (2010) Structure and function of mitochondrial supercomplexes. *BBA - Bioenergetics* **1797,** 664–670
15. Rydström Lundin, C., von Ballmoos, C., Ott, M., Ädelroth, P., and Brzezinski, P. (2016) Regulatory role of the respiratory supercomplex factors in *Saccharomyces cerevisiae*. *Proc. Natl. Acad. Sci. U.S.A.* **113,** E4476-E4485
16. Jiang, F., Ryan, M. T., Schlame, M., Zhao, M., Gu, Z., Klingenberg, M., Pfanner, N., and Greenberg, M. L. (2000) Absence of cardiolipin in the *crd1* null mutant results in decreased mitochondrial membrane potential and reduced mitochondrial function. *J. Biol. Chem.* **275,** 22387–22394
17. Zhang, M., Mileykovskaya, E., and Dowhan, W. (2002) Gluing the respiratory chain together: cardiolipin is required for supercomplex formation in the inner mitochondrial membrane. *J. Biol. Chem.* **277,** 43553–43556

18. Pfeiffer, K., Gohil, V., Stuart, R. A., Hunte, C., Brandt, U., Greenberg, M. L., and Schägger, H. (2003) Cardiolipin stabilizes respiratory chain supercomplexes. *J. Biol. Chem.* **278,** 52873–52880
19. Mileykovskaya, E., Zhang, M., and Dowhan, W. (2005) Cardiolipin in energy transducing membranes. *Biochemistry Mosc.* **70,** 154–158
20. Zhang, M., Mileykovskaya, E., and Dowhan, W. (2005) Cardiolipin is essential for organization of complexes III and IV into a supercomplex in intact yeast mitochondria. *J. Biol. Chem.* **280,** 29403–29408
21. Dienhart, M. K., and Stuart, R. A. (2008) The yeast Aac2 protein exists in physical association with the cytochrome bc_1-COX supercomplex and the TIM23 machinery. *Mol. Biol. Cell* **19,** 3934–3943
22. Chen, Y.-C., Taylor, E. B., Dephoure, N., Heo, J.-M., Tonhato, A., Papandreou, I., Nath, N., Denko, N. C., Gygi, S. P., and Rutter, J. (2012) Identification of a protein mediating respiratory supercomplex stability. *Cell Metab.* **15,** 348–360
23. Strogolova, V., Furness, A., Robb-McGrath, M., Garlich, J., and Stuart, R. A. (2012) Rcf1 and Rcf2, Members of the hypoxia-induced gene 1 protein family, are critical components of the mitochondrial cytochrome bc_1-cytochrome *c* oxidase supercomplex. *Mol. Cell Biol.* **32,** 1363–1373
24. Vukotic, M., Oeljeklaus, S., Wiese, S., Vögtle, F. N., Meisinger, C., Meyer, H. E., Zieseniss, A., Katschinski, D. M., Jans, D. C., Jakobs, S., Warscheid, B., Rehling, P., and Deckers, M. (2012) Rcf1 mediates cytochrome oxidase assembly and respirasome formation, revealing heterogeneity of the enzyme complex. *Cell Metab.* **15,** 336–347
25. Wang, J., Cao, Y., Chen, Y., Chen, Y., Gardner, P., and Steiner, D. F. (2006) Pancreatic cells lack a low glucose and O_2-inducible mitochondrial protein that augments cell survival. *Proc. Natl. Acad. Sci. U.S.A.* **103,** 10636–10641
26. Ameri, K., Rajah, A. M., Nguyen, V., Sanders, T. A., Jahangiri, A., Delay, M., Donne, M., Choi, H. J., Tormos, K. V., Yeghiazarians, Y., Jeffrey, S. S., Rinaudo, P. F., Rowitch, D. H., Aghi, M., and Maltepe, E. (2013) Nuclear localization of the mitochondrial factor HIGD1A during metabolic stress. *PLoS ONE* **8,** e62758–11
27. Ameri, K., Jahangiri, A., Rajah, A. M., Tormos, K. V., Nagarajan, R., Pekmezci, M., Nguyen, V., Wheeler, M. L., Murphy, M. P., Sanders, T. A., Jeffrey, S. S., Yeghiazarians, Y., Rinaudo, P. F., Costello, J. F., Aghi, M. K., and Maltepe, E. (2015) HIGD1A regulates oxygen consumption, ROS production, and AMPK activity during glucose deprivation to modulate cell survival and tumor growth. *Cell Rep.* 10.1016/j.celrep.2015.01.020
28. Strecker, V., Kadeer, Z., Heidler, J., Cruciat, C.-M., Angerer, H., Giese, H., Pfeiffer, K., Stuart, R. A., and Wittig, I. (2016) Supercomplex-associated Cox26 protein binds to cytochrome *c* oxidase. *BBA - Molecular Cell Research* **1863,** 1643–1652
29. Ogunjimi, E. O., Pokalsky, C. N., Shroyer, L. A., and Prochaska, L. J. (2000) Evidence for a conformational change in subunit III of bovine heart mitochondrial cytochrome *c* oxidase. *J. Bioenerg. Biomembr.* **32,** 617–626
30. Shinzawa-Itoh, K., Aoyama, H., Muramoto, K., Terada, H., Kurauchi, T., Tadehara, Y., Yamasaki, A., Sugimura, T., Kurono, S., Tsujimoto, K., Mizushima, T., Yamashita, E., Tsukihara, T., and Yoshikawa, S. (2007) Structures and physiological roles of 13 integral lipids of bovine heart cytochrome *c* oxidase. *EMBO J.* **26,** 1713–1725
31. Tamura, Y., Harada, Y., Nishikawa, S., Yamano, K., Kamiya, M., Shiota, T., Kuroda, T., Kuge, O., Sesaki, H., Imai, K., Tomii, K., and Endo, T. (2013) Tam41 Is a CDP-diacylglycerol synthase required for cardiolipin biosynthesis in mitochondria. *Cell Metab.* **17,** 709–718
32. Claypool, S. M., Boontheung, P., McCaffery, J. M., Loo, J. A., and Koehler, C. M. (2008) The cardiolipin transacylase, tafazzin, associates with two distinct respiratory components providing insight into Barth syndrome. *Mol. Biol. Cell* **19,** 5143–5155
33. Hayashi, T., Asano, Y., Shintani, Y., Aoyama, H., Kioka, H., Tsukamoto, O., Hikita, M., Shinzawa-Itoh, K., Takafuji, K., Higo, S., Kato, H., Yamazaki, S., Matsuoka, K., Nakano, A., Asanuma, H., *et al.* (2015) Higd1a is a positive regulator of cytochrome *c* oxidase. *Proc. Natl. Acad. Sci. U.S.A.* **112,** 1553–1558
34. Mileykovskaya, E., and Dowhan, W. (2014) Cardiolipin-dependent formation of mitochondrial respiratory supercomplexes. *Chem. Phys. Lipids* **179,** 42–48
35. Chen, X. J. (2004) Sal1p, a calcium-dependent carrier protein that suppresses an essential cellular function associated with the Aac2 isoform of ADP/ATP translocase in *Saccharomyces cerevisiae*. *Genetics* **167,** 607–617
36. Gallas, M. R., Dienhart, M. K., Stuart, R. A., and Long, R. M. (2006) Characterization of Mmp37p, a *Saccharomyces cerevisiae* mitochondrial matrix protein with a role in mitochondrial protein import. *Mol. Biol. Cell* **17,** 4051–4062
37. Jia, L., Dienhart, M. K., and Stuart, R. A. (2007) Oxa1 directly interacts with Atp9 and mediates its assembly into the mitochondrial F1Fo-ATP synthase complex. *Mol. Biol. Cell* **18,** 1897–1908
38. Heide, H., Bleier, L., Steger, M., Ackermann, J., Dröse, S., Schwamb, B., Zörnig, M., Reichert, A. S., Koch, I., Wittig, I., and Brandt, U. (2012) Complexome profiling identifies TMEM126B as a component of the mitochondrial complex I assembly complex. *Cell Metab.* **16,** 538–549
39. Cox, J., and Mann, M. (2008) MaxQuant enables high peptide identification rates, individualized p.p.b.-range mass accuracies and proteome-wide protein quantification. *Nat. Biotechnol.* **26,** 1367–1372
40. Hell, K., Neupert, W., and Stuart, R. A. (2001) Oxa1p acts as a general membrane insertion machinery for proteins encoded by mitochondrial DNA. *EMBO J.* **20,** 1281–1288
41. Laemmli, U. K. (1970) Cleavage of structural proteins during the assembly of the head of bacteriophage T4. *Nature* **227,** 680–685
42. Bradford. (1976) A rapid and sensitive method for the quantitation of microgram quantities of protein utilizing the principle of protein-dye binding. *Anal. Biochem.* **72,** 248–254